Geophysical Research Letters

RESEARCH LETTER
10.1029/2019GL084047

Key Points:
- Aerosol hygroscopicity changes quickly between clean and polluted periods in Beijing
- Ultrafine-mode particles stem chiefly from nucleation in clean environments and from primary emissions in polluted environments
- Ultrafine- and accumulation-mode particles have distinct properties in urban environments

Supporting Information:
- Supporting Information S1

Correspondence to:
Z. Li,
zli@atmos.umd.edu

Citation:
Wang, Y., Li, Z., Zhang, R., Jin, X., Xu, W., Fan, X., et al (2019). Distinct ultrafine- and accumulation-mode particle properties in clean and polluted urban environments. *Geophysical Research Letters*, *46*, 10,918–10,925. https://doi.org/10.1029/2019GL084047

Received 10 JUN 2019
Accepted 5 SEP 2019
Accepted article online 11 SEP 2019
Published online 15 OCT 2019

Distinct Ultrafine- and Accumulation-Mode Particle Properties in Clean and Polluted Urban Environments

Yuying Wang[1,2], Zhanqing Li[3], Renyi Zhang[4], Xiaoai Jin[2], Weiqi Xu[5], Xinxin Fan[2], Hao Wu[2], Fang Zhang[2], Yele Sun[5], Qiuyan Wang[1], Maureen Cribb[3], and Dawei Hu[6]

[1]Key Laboratory for Aerosol-Cloud-Precipitation of China Meteorological Administration, Nanjing University of Information Science and Technology, Nanjing, China, [2]State Key Laboratory of Remote Sensing Sciences, College of Global Change and Earth System Science, Beijing Normal University, Beijing, China, [3]ESSIC and the Department of Atmospheric and Oceanic Science, University of Maryland, College Park, MD, USA, [4]Department of Atmospheric Sciences and Department of Chemistry, Center for Atmospheric Chemistry and Environment, Texas A&M University, College Station, TX, USA, [5]State Key Laboratory of Atmospheric Boundary Layer Physics and Atmospheric Chemistry, Institute of Atmospheric Physics, Chinese Academy of Sciences, Beijing, China, [6]School of Earth and Environmental Sciences, University of Manchester, Manchester, UK

Abstract In this study, we report the phenomenon of fast changes in aerosol hygroscopicity between clean and polluted periods observed frequently in urban Beijing during winter using a hygroscopicity tandem mobility analyzer. The cause of this phenomenon and the formation process of particles in different modes are discussed. During clean periods, ultrafine-mode particles (i.e., nucleation and Aitken modes) stem mainly from nucleation events with subsequent growth. During heavily polluted periods, ultrafine-mode particles originate chiefly from primary emissions. Larger-mode particles like accumulation-mode particles are mainly from primary emissions during clean periods and aqueous reactions during polluted periods. This finding based on hygroscopicity tandem mobility analyzer measurements can make up the deficiency of mass-dependent instruments in analyzing sources and chemical processes of ultrafine-mode particles.

Plain Language Summary The mass concentration of ultrafine-mode particles in the atmosphere is extremely low, and their properties are rarely investigated using instruments specialized in measuring such things. The hygroscopicity tandem mobility analyzer makes it possible to study sources and chemical processes of ultrafine-mode particles. They were measured in terms of aerosol number concentration, and aerosol hygroscopicity indirectly reflects aerosol chemical compositions. The properties of ultrafine- and accumulation-mode particles differed considerably between clean and polluted urban environments. Investigated were their different formation processes.

1. Introduction

Beijing, the capital city of China, experiences severe air pollution events every year, especially during the winter season. To investigate the mechanism of haze formation, many field campaigns have been conducted in Beijing and surrounding areas (Y. J. Li et al., 2017; Z. Li et al., 2017). Some studies have reported that high emissions and a strong atmospheric oxidation capacity are the major causes for particle formation followed by rapid growth in this region (Guo et al., 2014; Wang et al., 2017). Secondary organic and inorganic compounds are found more frequently than compounds characteristic of primary emissions during periods of haze formation (Huang et al., 2014; Y. J. Li, Sun, et al., 2017). Some other studies have suggested that aqueous chemical reactions are important for particle growth and accumulation (e.g., Cheng et al., 2016; G. Wang et al., 2016; Z. Wang et al., 2016; Wu et al., 2018). The majority of these studies are based on analyzes of bulk chemical mass concentrations of PM_1 or $PM_{2.5}$ (i.e., total particle matters with diameters less than 1 or 2.5 micrometer, respectively). The mass concentration of particles in the nucleation and Aitken modes with diameters (D_p) less than 100 nm contributes very little to PM_1 and $PM_{2.5}$, although their number concentrations are always high. Their chemical species of these ultrafine-mode particles are hard to be measured accurately during field campaigns because their mass concentrations are below the observation limits of the majority of mass-dependent instruments such as the aerosol mass spectrometer. It has thus been a major challenge to understand the chemical processes in PM_1 or $PM_{2.5}$ for nucleation- and Aitken-mode particles.

Investigating the source and chemical compositions of the ultrafine-mode (D_p < 100 nm) particles is important because these ultrafine-mode particles are plentiful and can grow to large particles during pollution haze episodes (Guo et al., 2014).

The hygroscopicity tandem differential mobility analyzer (H-TDMA) makes it possible to estimate aerosol chemical compositions indirectly based on the particle hygroscopicity (Swietlicki et al., 2008; Ye et al., 2011; Zhang et al., 2017). The hygroscopic growth factor (GF) is defined as the ratio of the wet diameter at a certain relative humidity (RH) and to the dry diameter. GFs for different chemical species differ drastically (Petters & Kreidenweis, 2007). The H-TDMA can measure the GF probability distribution function (GF-PDF) for particles with a specified diameter. Detailed information on the aerosol hygroscopicity conveyed in the measurements of the H-TDMA can be used to study aerosol sources (Y. Wang et al., 2018; Xie et al., 2017). This is because the GF-PDF pattern depends on aerosol chemical composition and the mixing state, both of which are highly related to aerosol formation and aging processes (Liu et al., 2011; Wang et al., 2017). H-TDMA measurements are based on the aerosol number concentration, which is high when D_p < 100 nm. Therefore, the H-TDMA can make up the deficiency of mass-dependent instruments in studying the properties of ultrafine-mode particles.

Petters and Kreidenweis (2007) proposed a single hygroscopicity parameter (κ). It can be retrieved by GF at a certain RH, and the κ-probability distribution function (κ-PDF) can be retrieved from the GF-PDF (Y. Wang et al., 2017). There are always two modes in the GF-PDF or κ-PDF for 40- to 200-nm particles in Beijing (Y. Wang et al., 2017; Figure S1a in the supporting information): one less-hygroscopic (LH) mode and one more-hygroscopic (MH) mode. The GF peak value of separating two modes is around 1.2 (κ_{peak} = 0.1). LH-mode particles in urban environments are mainly composed of hydrophobic compounds such as externally mixed black carbon (BC), organics, or their mixtures. MH-mode particles are mainly composed of hydrophilic compounds such as some secondary organics and secondary inorganics (sulfate, nitrate, and ammonium salts) or their mixture with primarily emitted species (Wu et al., 2016; Müller et al., 2017; Y. Wang et al., 2017). In other words, LH-mode particles are mainly from primary emissions, while the MH-mode particles are mainly from secondary formation or the aging of primary particles (Figure S1b). LH- and MH-mode particles thus represent different aerosol sources and chemical processes. Implied aerosol chemical information from the GF-PDF/κ-PDF can be used to analyze particle formation processes for particles of different sizes, which is necessary to study the haze formation mechanism (X. Wang et al., 2018; Xie et al., 2017).

This study examines aerosol properties based on H-TDMA measurements and compares the measurement results of mass-dependent instruments. Proposed are different formation mechanisms of differently sized mode particles for clean and polluted episodes in an urban environment.

2. Experiment

2.1. The H-TDMA System

The H-TDMA system used in this study was custom built (Tan et al., 2013; Y. Wang, Li, et al., 2018). Briefly, this system mainly includes two differential mobility analyzers (DMA, model 3081L, TSI Inc.) and a water-based condensation particle counter (WCPC, model 3787, TSI Inc.). The dried and neutralized aerosol sample passes through the first DMA, which selects monodispersed particles of a certain diameter, then goes through a Nafion humidifier to humidify the sample. Finally, the sample passes through the second DMA and the WCPC to measure the number size distribution of the humidified particles. The dry diameters selected by the first DMA were 40, 80, 110, 150, and 200 nm, and the humidified RH was set to 90%. The GF is expressed mathematically as

$$\mathrm{GF} = \frac{D_p(\mathrm{RH})}{D_d}, \tag{1}$$

where D_p(RH) is the particle diameter at the given RH and D_d is the dry diameter selected by the first DMA. WCPC data can be used to calculate the GF measured distribution function. The GF-PDF is then retrieved using the multimode TDMAfit algorithm (Stolzenburg & McMurry, 2008). This algorithm separates the LH and MH modes. The hygroscopicity parameter (κ) is calculated following Petters and Kreidenweis (2007):

$$\kappa = \left(\mathrm{GF}^3 - 1\right) \cdot \left[\frac{1}{\mathrm{RH}} \exp\left(\frac{4\sigma_{s/a} M_w}{RT\rho_w D_d \mathrm{GF}}\right) - 1\right], \quad (2)$$

where $\sigma_{s/a}$ is the surface tension coefficient, M_w is the mole mass of water, R is the universal gas constant, T is the temperature, and ρ_w is the density of water.

2.2. Field Campaign and Instruments

Measurements used in this study were collected from 15 November 2016 to 13 December 2016 during the Air Pollution and Human Health winter field campaign that took place at the observation site of the Institute of Atmospheric Physics, Chinese Academy of Sciences (39.97°N, 116.37°E, 49 m above sea level) between the third and fourth ring roads in urban Beijing, China. The meteorological parameters measured include wind direction, wind speed, RH, and T at the 8- and 280-m levels of the Beijing 325-m meteorological tower. An Aerodyne quadrupole aerosol chemical speciation monitor, described in detail by Ng et al. (2011), measured the mass concentrations of nonrefractory chemical species in PM_1. A multiwavelength aethalometer (Model AE33, Magee Scientific Corp.) measured the mass concentration of BC. A scanning mobility particle sizer equipped with a long DMA (model 3081L, TSI Inc.) and a condensation particle counter (model 3772, TSI Inc.) measured the aerosol particle number size distribution (13–552 nm). All instruments were calibrated before and after the field campaign.

3. Results

3.1. Overview

Figure 1 shows the time series of the meteorological parameters, the aerosol chemical species in PM_1, and GF-PDFs. Based on these measurements, several clean and polluted periods were chosen during this campaign according to the wind direction and PM_1 mass concentration (Figure 1). The mean PM_1 mass concentrations were 12.8 and 130.7 $\mu g/m^3$ during the clean and polluted periods. Changes in the wind direction from strong northerly winds to light southerly winds induced the rapid transition between clean and polluted periods (Figure 1a). Southerly winds push the air mass through the bulk of Beijing, ushering in more pollutants from the more populated areas to the south where many heavy industries are located to the site north of central Beijing. This southerly flow from warmer regions to the south as well as from the ocean has a higher water content. Strong northerly winds disperse accumulation-mode particles, enabling nucleation events, while light southerly winds favor aerosol growth and accumulation (Guo et al., 2014; Sun, Chen, et al., 2016).

Figure 2 shows the size-resolved mean number fraction of the LH mode (NF_{LH}) and mean GF (GF_m) for particles at this site. The NF_{LH} of 40-nm particles is higher during polluted periods than during clean periods, while the NF_{LH} of 80- to 200-nm particles shows the reverse trend. This suggests that 40- and 80- to 200-nm particles have different chemical compositions. Figure 2 also shows smaller GF_m for 40-nm particles and larger GF_m for 80- to 200-nm particles during the polluted periods than the clean periods. The opposite trends in GF_m and NF_{LH} between 40- and 80- to 200-nm particles imply different sources and chemical processes of them. This difference is hard to be analyzed using mass-based instruments.

Ultrafine particles (i.e. nucleation- and Aitken-mode particles) are the 40-nm particles, and large particles (i.e., accumulation-mode particles) are the 150-nm particles in this study for the purpose of discussing their different sources and chemical processes. The sharp changes in aerosol properties between clean and polluted periods are also visible in the time series of particle number size distribution (Figure 1b), chemical species in PM_1 (Figure 1c), and 150- and 40-nm GF-PDFs (Figures 1d and 1e). To illustrate the transition process between clean and polluted periods and its impact on aerosol properties, two cases are analyzed (Figure 1): a polluted-to-clean transition case (Case 1) and a clean-to-polluted transition case (Case 2).

Case 1. Mean PM_1 mass concentrations were 239.8 and 36.8 $\mu g/m^3$ during the polluted and clean periods. Ambient RH levels were 51.5% (polluted) and 26.6% (clean). The 150- and 40-nm GF-PDF patterns shifted during the quick transition from polluted to clean periods at ~01:00 local time (LT) on 27 November 2016. Compared with the polluted period, the LH mode of 150-nm particles strengthened and MH mode

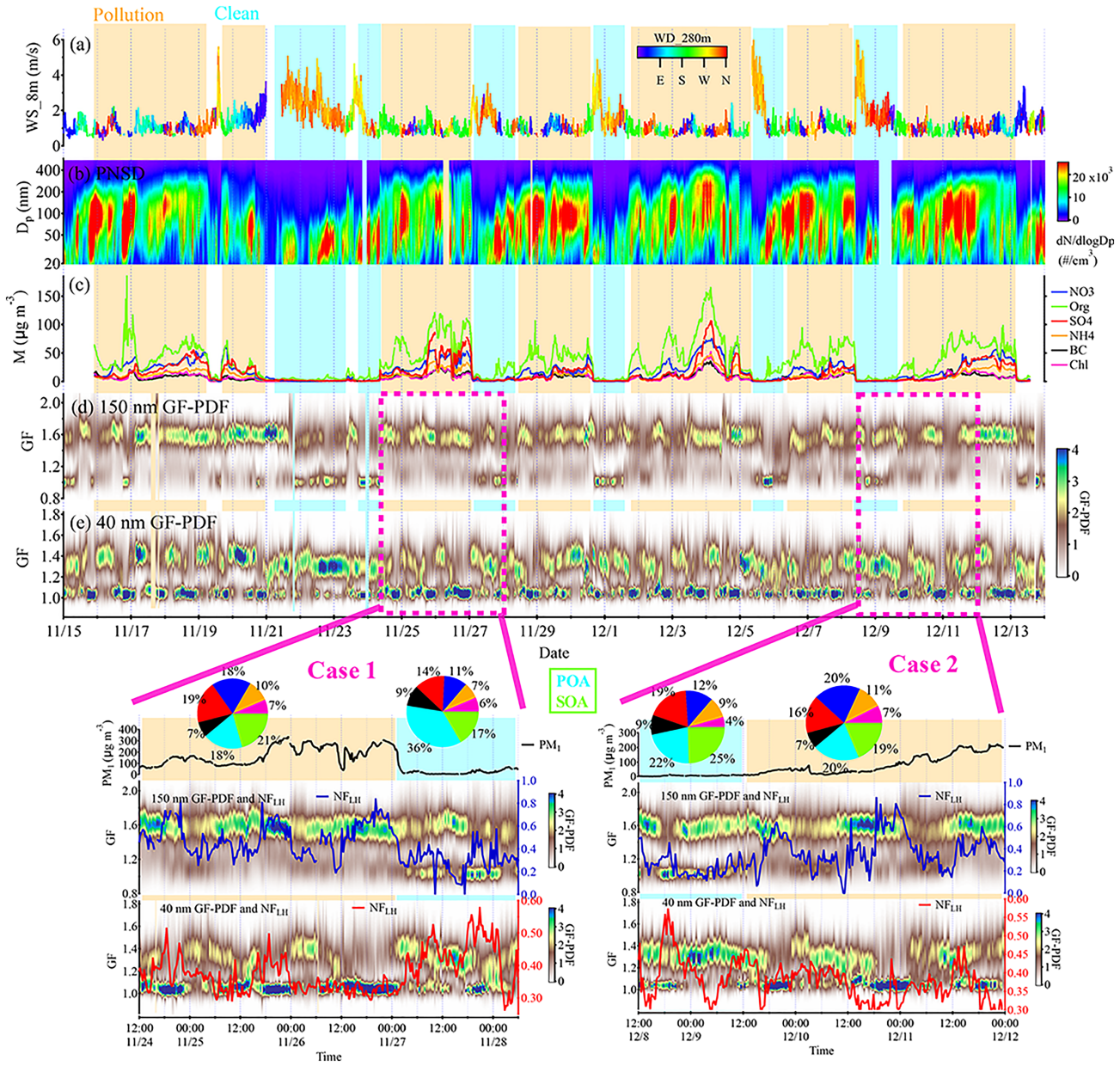

Figure 1. Time series of (a) wind direction (WD) at 280 m and wind speed (WS) at 8 m above ground level, (b) particle number size distribution (PNSD) measured by the scanning mobility particle sizer, (c) mass concentrations of chemical species in PM_1 measured by Aerosol Chemical Speciation Monitor and aethalometer (Chl in the legend refers to chorine salt), (d, e) hygroscopic growth factor distributions (GF-PDF) for 150- and 40-nm particles measured by the hygroscopicity tandem differential mobility analyzer. Clean and Pollution periods are marked in (a)–(e). Cases 1 and 2 panels show time series of PM_1, GF-PDF, and the number fraction of the less-hygroscopic mode (NF_{LH}) of 40- and 150-nm particles. The pie charts show the mass fractions of different chemical species in PM_1 during the corresponding clean or polluted periods. SOA = secondary organic aerosol; POA = primary organic aerosol; PM = particle matters.

weakened during the clean period. The GF-PDF pattern of 40-nm particles is opposite of that of 150-nm particles, that is, a weaken LH mode and an enhanced MH mode during the clean period. From polluted to clean periods, the NF_{LH} of the 40-nm particles decreased from 0.50 to 0.31, while that of the 150-nm particles increased from 0.36 to 0.43. This suggests that there are fewer particles in the hydrophobic nucleation and Aitken modes but more in the hydrophobic accumulation mode during clean periods than during polluted periods. PM_1 chemical mass fractions show more hydrophobic compounds (primary organic aerosols and BC) during clean periods than during polluted periods (25% to 44%). This can be

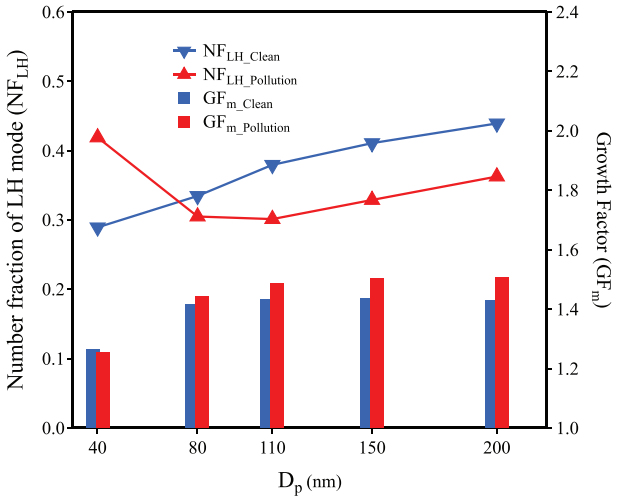

Figure 2. Size-resolved number fraction of less-hygroscopic mode particles (NF_{LH}) and mean growth factor (GF) during clean (blue) and polluted (red) periods.

used to interpret the variation in NF_{LH} of accumulation-mode particles but not that of nucleation- and Aitken-mode particles.

Case 2. Mean PM_1 concentrations were 12.6 and 127.5 μg/m^3 during the clean and polluted periods, respectively. Ambient RH levels were 27.9% (clean) and 43.6% (polluted). As in Case 1, the GF-PDF pattern of 150-nm particles has a weaker LH mode and stronger MH mode during polluted periods than during clean periods. The GF-PDF pattern of the 40-nm particles is also opposite of that of the 150-nm particles, that is, a weaken LH mode and an enhanced MH mode during the clean period. From clean to polluted periods, the NF_{LH} of 40-nm particles increased from 0.24 to 0.38 and that of the 150-nm particles decreased from 0.40 to 0.36. The hydrophobic compositions in PM_1 decreased from 31% to 27%.

In summary, the GF-PDF patterns point to different transitions for ultrafine- and accumulation-mode particles between clean and polluted periods. The decrease in hydrophobic compounds in PM_1 during polluted periods is synchronous with the decrease in the LH mode of large particles (such as 150-nm particles) but not with that of ultrafine particles (such as 40-nm particles). This implies that the PM_1 chemical mass concentration measured by the Aerosol Chemical Speciation Monitor and the aethalometer can reflect the variations in the chemical composition of accumulation-mode particles but not nucleation- and Aitken-mode particles.

3.2. Diurnal Variations in κ-PDF and NF_{LH}

The κ-PDF patterns of 40-nm particles during clean and polluted periods differ (Figures 3a and 3b). As reported by others (e.g., Peng et al., 2014; Wang et al., 2017), 40-nm particles are mainly from the growth of newly formed particles or primary emissions (i.e., local-impacted particles). During the clean periods of this field campaign, new particle formation (NPF) events occurred frequently (Figures 1b and S2). During NPF, the 40-nm particles appeared in large numbers at ~12:00 LT, and the κ-PDF of these particles showed an enhanced MH mode and a weakened LH mode. Figure 3e shows that the NF_{LH} of 40-nm particles was less than 0.5 in any time of day. And NF_{LH} of 40-nm particles decreased from ~0.4 at 12:30 LT to ~0.2 at 14:30 LT. Simultaneously, the mean κ in the MH mode (κ_{m_MH}) increased slightly from 0.19 to 0.20 (Figure 3a), which is lower than κ for ammonium sulfate ($\kappa_{(NH4)2SO4} = 0.48$) but larger than that for secondary organics ($\kappa_{SOA} = 0.10$). These results suggest that during clean periods, the daytime increase in 40-nm particles is mainly from NPF and that more hydrophilic compounds are formed through the photochemical reactions and condensations by the oxidation products from gas precursors (SO_2 and volatile organic compounds). Zheng et al. (2011) reported that the condensation of gaseous sulfuric acid (followed by neutralization with ammonia) dominates particle growth in the Aitken-mode particles in urban Beijing. At about 16:30 LT, NF_{LH} increased again and peaked at 19:30 LT, while both κ_{m_MH} and κ_{m_LH} had slight decreases (Figure 3a). This is likely related to primary sources, including vehicle exhaust and cooking emissions. Wang et al. (2017) found that 40-nm particles from local sources in Beijing are hydrophobic. The κ-PDF diurnal variations of 40-nm particles during polluted and clean periods differ (Figure 3b). The MH mode weakens, and the LH mode strengthens during the day. NF_{LH} has three peaks (Figure 3f), corresponding to three cooking and rush hours. This suggests that primary emissions are the dominant sources of 40-nm particles during polluted periods.

The κ-PDFs of 150-nm particles during clean and polluted periods had similar diurnal variation patterns with some differences (Figures 3c and 3d). First, κ_{m_MH} is lower during clean periods than during polluted periods, especially at night. Second, NF_{LH} is higher during clean periods than during polluted periods. The diurnal variation pattern of NF_{LH} during clean periods also exhibits three peaks corresponding to three cooking and rush hours (Figure 3e), while that during polluted periods varies slightly. These results suggest that 150-nm particles are influenced by local primary emissions during clean periods. The low and almost invariable NF_{LH} (Figure 3f) during polluted periods suggests that most of the 150-nm particles are internally mixed and highly aged. This is likely related to heterogeneous reactions on the particles' surface.

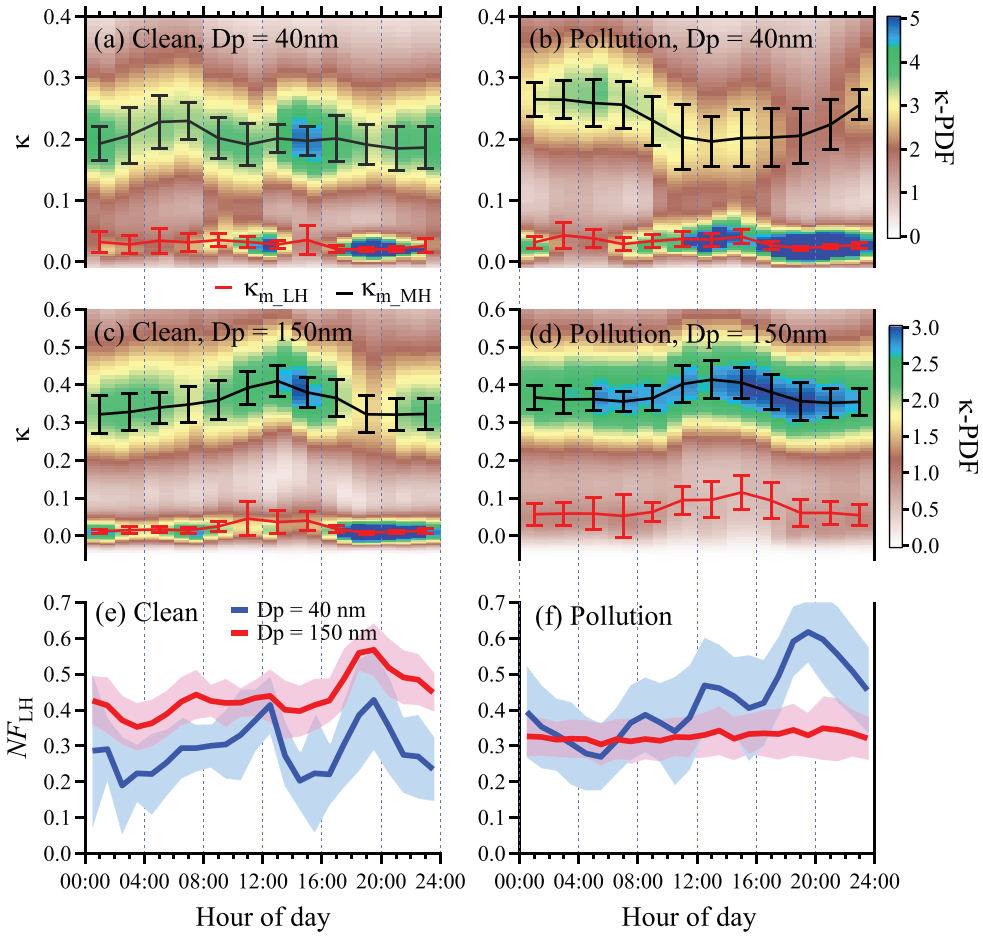

Figure 3. Diurnal variations in κ-probability distribution function (PDF) for 40-nm particles during (a) clean and (b) polluted periods, κ-PDF for 200-nm particles during (c) clean and (d) polluted periods, and the number fraction of the less-hygroscopic mode (NF_{LH}) for (e) 40- and (f) 150-nm particles. The black and red lines in (a) and (b) are the mean κ of the more-hygroscopic (MH) and less-hygroscopic (LH) modes (i.e., κ_{m_MH} and κ_{m_LH}) in κ-PDF. The error bars represent the standard deviations of corresponding parameters.

4. Hypothesis About the Underlying Mechanisms

As shown in previous sections, significant differences in aerosol hygroscopicity exist between 40- and 150-nm particles during clean and polluted periods. This suggests different sources and chemical processes for the ultrafine- and accumulation-mode particles. Figure S4 shows one possible interpretation.

During clean periods, more solar radiation reaches the ground, and ambient RH is low. The high actinic flux and lower surface area of preexisting particles (Figure S5) increase gaseous sulfuric acid concentrations (Zheng et al., 2011), which is the main cause of NPF events and the subsequent growth of particles in urban Beijing (Yue et al., 2010). In other words, daytime ultrafine-mode particles are mainly from photochemical reactions due to the high-atmospheric oxidation capacity (Figure S6). Most newly formed particles through photochemical reaction are mixed internally with high hygroscopicities (Wang et al., 2017; Wu et al., 2016). This causes the decreased NF_{LH} and enhanced κ_{m_MH} for 40-nm particles, especially in the afternoon. The number concentration of accumulation-mode particles is low (Figure S2) during clean periods, and these particles are mainly from primary emission, which consists of many externally mixed hydrophobic species (Y. Wang et al., 2017). This is why the enhanced NF_{LH} of 150-nm particles and its peaks correspond to three rush hours.

During polluted periods, less solar radiation reaches the ground, and ambient RH is high. Aqueous reactions on the particle surface play an important role in aerosol growth (Sun, Du, et al., 2016). The aqueous oxidation

of SO_2 by NO_2 leads to large sulfate production rates, and the increased aerosol liquid water further promotes the formation of nitrate and secondary organic aerosol through other aqueous chemical processes, making particles quickly aged in polluted environments (e.g., Sun, Du, et al., 2016; G. Wang, Zhang, et al., 2016; Wu et al., 2018). Internally mixed accumulation-mode particles are thus abundant and have high hygroscopicities. Ultrafine-mode particles during polluted periods are mainly from primary emissions due to weak photochemical reactions. This is why 40-nm particles have weaker hygroscopicities and increased NF_{LH} in the daytime. Coagulation of these ultrafine-mode particles by large particles can occur. These ultrafine-mode particles can also grow quickly through aqueous chemical reactions, which clearly occurs at night when ambient RH levels can exceed 60% (Figures S2 and S3).

5. Conclusions and Summary

During the Air Pollution and Human Health winter field campaign in Beijing in 2016, the phenomenon of drastic changes in aerosol hygroscopicity between clean and polluted periods was observed frequently using a hygroscopicity tandem mobility analyzer system. The direction of the change was opposite between ultrafine (nucleation and Aitken modes) and larger (accumulation mode) particles. The variations in the chemical composition of PM_1 between clean and polluted periods can be used to interpret the variation in hygroscopicity of large particles but not of ultrafine particles, pointing to a limitation of mass-dependent instruments to study the sources and chemical processes of ultrafine particles.

One LH mode and one MH mode in the GF/κ-PDF patterns represent different particle formation and aging processes in urban environments, which are used to further analyze the aerosol sources of differently sized particles in this study. The aerosol hygroscopicity of accumulation-mode particles during haze episodes was influenced largely by heterogeneous reactions (such as aqueous reactions), consistent with previous findings based on mass-dependent instruments. However, ultrafine-mode particles are mainly from NPF events followed by more growth during clean periods but are mainly from primary emission during polluted periods in urban environments.

Acknowledgments
This work was funded by the National Key R&D Program of the Ministry of Science and Technology, China (Grant 2017YFC1501702), the National Natural Science Foundation of China (NSFC) research project (Grant 91544217), the Startup Foundation for Introducing Talent of NUIST, and the China Scholarship Council (Award 201706040194). We thank all participants in the field campaign for their tireless work and cooperation. The associated data can be downloaded online (https://pan.baidu.com/s/1p1iNAeYuB0crF934l2FzlQ).

References

Cheng, Y., Zheng, G., Wei, C., Mu, Q., Zheng, B., Wang, Z., et al. (2016). Reactive nitrogen chemistry in aerosol water as a source of sulfate during haze events in China. *Science Advances*, *2*(12). https://doi.org/10.1126/sciadv.1601530

Guo, S., Hu, M., Zamora, M. L., Peng, J., Shang, D., Zheng, J., et al. (2014). Elucidating severe urban haze formation in China. *Proceedings of the National Academy of Sciences*, *111*(49), 17,373–17,378. https://doi.org/10.1073/pnas.1419604111

Huang, R. J., Zhang, Y., Bozzetti, C., Ho, K. F., Cao, J. J., Han, Y., et al. (2014). High secondary aerosol contribution to particulate pollution during haze events in China. *Nature*, *514*(7521), 218–222. https://doi.org/10.1038/nature13774

Li, Y. J., Sun, Y., Zhang, Q., Li, X., Li, M., Zhou, Z., & Chan, C. K. (2017). Real-time chemical characterization of atmospheric particulate matter in China: A review. *Atmospheric Environment*, *158*, 270–304. https://doi.org/10.1016/j.atmosenv.2017.02.027

Li, Z., Guo, J., Ding, A., Liao, H., Liu, J., Sun, Y., et al. (2017). Aerosol and boundary-layer interactions and impact on air quality. *National Science Review*, *4*(6), 810–833. https://doi.org/10.1093/nsr/nwx117

Liu, P. F., Zhao, C. S., Göbel, T., Hallbauer, E., Nowak, A., Ran, L., et al. (2011). Hygroscopic properties of aerosol particles at high relative humidity and their diurnal variations in the North China Plain. *Atmospheric Chemistry and Physics*, *11*(7), 3479–3494. https://doi.org/10.5194/acp-11-3479-2011

Müller, A., Miyazaki, Y., Aggarwal, S. G., Kitamori, Y., Boreddy, S. K., & Kawamura, K. (2017). Effects of chemical composition and mixing state on size-resolved hygroscopicity and cloud condensation nuclei activity of submicron aerosols at a suburban site in northern Japan in summer. *Journal of Geophysical Research: Atmospheres*, *122*, 9301–9318. https://doi.org/10.1002/2017JD027286

Ng, N. L., Herndon, S. C., Trimborn, A., Canagaratna, M. R., Croteau, P. L., Onasch, T. B., et al. (2011). An Aerosol Chemical Speciation Monitor (ACSM) for routine monitoring of the composition and mass concentrations of ambient aerosol. *Aerosol Science and Technology*, *45*(7), 780–794. https://doi.org/10.1080/02786826.2011.560211

Peng, J. F., Hu, M., Wang, Z. B., Huang, X. F., Kumar, P., Wu, Z. J., et al. (2014). Submicron aerosols at thirteen diversified sites in China: Size distribution, new particle formation and corresponding contribution to cloud condensation nuclei production. *Atmospheric Chemistry and Physics*, *14*(18), 10,249–10,265. https://doi.org/10.5194/acp-14-10249-2014

Petters, M. D., & Kreidenweis, S. M. (2007). A single parameter representation of hygroscopic growth and cloud condensation nucleus activity. *Atmospheric Chemistry and Physics*, *7*(8), 1961–1971. https://doi.org/10.5194/acp-7-1961-2007

Stolzenburg, M. R., & McMurry, P. H. (2008). Equations governing single and tandem DMA configurations and a new lognormal approximation to the transfer function. *Aerosol Science and Technology*, *42*(6), 421–432. https://doi.org/10.1080/02786820802157823

Sun, Y., Chen, C., Zhang, Y., Xu, W., Zhou, L., Cheng, X., et al. (2016). Rapid formation and evolution of an extreme haze episode in Northern China during winter 2015. *Scientific Reports*, *6*(1), 27,151. https://doi.org/10.1038/srep27151

Sun, Y., Du, W., Fu, P., Wang, Q., Li, J., Ge, X., et al. (2016). Primary and secondary aerosols in Beijing in winter: Sources, variations and processes. *Atmospheric Chemistry and Physics*, *16*(13), 8309–8329. https://doi.org/10.5194/acp-16-8309-2016

Swietlicki, E., Hansson, H. . C., Hämeri, K., Svenningsson, B., Massling, A., Mcfiggans, G., et al. (2008). Hygroscopic properties of submicrometer atmospheric aerosol particles measured with H-TDMA instruments in various environments—A review. *Tellus Series B: Chemical and Physical Meteorology*, *60*(3), 432–469. https://doi.org/10.1111/j.1600-0889.2008.00350.x

Tan, H., Xu, H., Wan, Q., Li, F., Deng, X., Chan, P. W., et al. (2013). Design and application of an unattended multifunctional H-TDMA system. *Journal of Atmospheric and Oceanic Technology*, *30*(6), 1136–1148. https://doi.org/10.1175/jtech-d-12-00129.1

Wang, G., Zhang, R., Gomez, M. E., Yang, L., Levy Zamora, M., Hu, M., et al. (2016). Persistent sulfate formation from London Fog to Chinese haze. *Proceedings of the National Academy of Sciences*, *113*(48), 13,630–13,635. https://doi.org/10.1073/pnas.1616540113

Wang, X., Shen, X. J., Sun, J. Y., Zhang, X. Y., Wang, Y. Q., Zhang, Y. M., et al. (2018). Size-resolved hygroscopic behavior of atmospheric aerosols during heavy aerosol pollution episodes in Beijing in December 2016. *Atmospheric Environment*, *194*, 188–197. https://doi.org/10.1016/j.atmosenv.2018.09.041

Wang, Y., Li, Z., Zhang, Y., du, W., Zhang, F., Tan, H., et al. (2018). Characterization of aerosol hygroscopicity, mixing state, and CCN activity at a suburban site in the central North China Plain. *Atmospheric Chemistry and Physics*, *18*(16), 11,739–11,752. https://doi.org/10.5194/acp-18-11739-2018

Wang, Y., Zhang, F., Li, Z., Tan, H., Xu, H., Ren, J., et al. (2017). Enhanced hydrophobicity and volatility of submicron aerosols under severe emission control conditions in Beijing. *Atmospheric Chemistry and Physics*, *17*(8), 5239–5251. https://doi.org/10.5194/acp-17-5239-2017

Wang, Z., Wu, Z., Yue, D., Shang, D., Guo, S., Sun, J., et al. (2016). New particle formation in China: Current knowledge and further directions. *Science of the Total Environment*, *577*, 258–266. https://doi.org/10.1016/j.scitotenv.2016.10.177

Wu, Z. J., Wang, Y., Tan, T., Zhu, Y., Li, M., Shang, D., et al. (2018). Aerosol liquid water driven by anthropogenic inorganic salts: Implying its key role in haze formation over the North China Plain. *Environmental Science & Technology Letters*, *5*(3), 160–166. https://doi.org/10.1021/acs.estlett.8b00021

Wu, Z. J., Zheng, J., Shang, D. J., du, Z. F., Wu, Y. S., Zeng, L. M., et al. (2016). Particle hygroscopicity and its link to chemical composition in the urban atmosphere of Beijing, China, during summertime. *Atmospheric Chemistry and Physics*, *16*(2), 1123–1138. https://doi.org/10.5194/acp-16-1123-2016

Xie, Y., Ye, X., Ma, Z., Tao, Y., Wang, R., Zhang, C., et al. (2017). Insight into winter haze formation mechanisms based on aerosol hygroscopicity and effective density measurements. *Atmospheric Chemistry and Physics*, *17*(11), 7277–7290. https://doi.org/10.5194/acp-17-7277-2017

Ye, X., Ma, Z., Zhang, J., Du, H., Chen, J., Chen, H., et al. (2011). Important role of ammonia on haze formation in Shanghai. *Environmental Research Letters*, *6*(2), 024019. https://doi.org/10.1088/1748-9326/6/2/024019

Yue, D. L., Hu, M., Zhang, R. Y., Wang, Z. B., Zheng, J., Wu, Z. J., et al. (2010). The roles of sulfuric acid in new particle formation and growth in the mega-city of Beijing. *Atmospheric Chemistry and Physics*, *10*(10), 4953–4960. https://doi.org/10.5194/acp-10-4953-2010

Zhang, F., Wang, Y., Peng, J., Ren, J., Collins, D., Zhang, R., et al. (2017). Uncertainty in predicting CCN activity of aged and primary aerosols. *Journal of Geophysical Research: Atmospheres*, *122*, 11,723–11,736. https://doi.org/10.1002/2017JD027058

Zheng, J., Hu, M., Zhang, R., Yue, D., Wang, Z., Guo, S., et al. (2011). Measurements of gaseous H_2SO_4 by AP-ID-CIMS during CAREBeijing 2008 Campaign. *Atmospheric Chemistry and Physics*, *11*(15), 7755–7765. https://doi.org/10.5194/acp-11-7755-2011